Original Article

DOI: 10.5582/bst.2019.01185

GRIM-19 over-expression represses the proliferation and invasion of orthotopically implanted hepatocarcinoma tumors associated with downregulation of Stat3 signaling

Dexia Kong[1,§], Junyu Chen[2,§], Xun Sun[3], Yan Lin[1], Yanwei Du[4], Di Huang[4], Hongjing Cheng[3], Ping He[3], Luoluo Yang[3], Shan Wu[2], Lijing Zhao[5,*], Xiangwei Meng[3,*]

[1] *Department of Gastroenterology, Zhejiang Provincial People's Hospital, People's Hospital of Hangzhou Medical College, Hangzhou, China;*
[2] *Department of Gynaecology and Obstetrics, Second Hospital of Jilin University, Changchun, China;*
[3] *Department of Gastroenterology, First Hospital of Jilin University, Changchun, China;*
[4] *Department of Pathophysiology, Basic Medicine School of Jilin University, Changchun, China;*
[5] *Department of Recovery, Nursing School of Jilin University, Changchun, China.*

Summary **The retinoid-interferon-induced mortality-19 (GRIM-19) gene has been identified as a negative regulator associated with tumor development. The current study created a model of an orthotopically implanted hepatocarcinoma tumor to verify the inhibitory effect of GRIM-19 *in vivo*. After treatment with GRIM-19 carried by attenuated *Salmonella*, transplanted tumors were measured with an Imaging System. The expression of GRIM-19, Stat3/p-Stat3, cyclinD1, CDK4, PCNA, Bax/Bcl-2, cleaved caspase-9/3, VEGF, and MMP-2/9 was determined using immunohistochemistry and Western blot analysis. The cell cycle was assessed using flow cytometry (FCM). Apoptosis was determined using FCM and a TUNEL assay. Results indicated that GRIM-19 overexpression resulted in inhibition of peritoneal metastasis, induction of cell cycle arrest, and apoptosis *in vivo*. In addition, the expression of Stat3/p-Stat3 was down-regulated by GRIM-19. These results suggest that GRIM-19 overexpression could suppress the growth of orthotopically implanted hepatocarcinoma tumors by reversing the regulation of the Stat3 signaling pathway. This approach could potentially be a powerful treatment for hepatocarcinoma.**

Keywords: GRIM-19, hepatocellular carcinoma, orthotopically implanted tumor, Stat3, apoptosis

1. Introduction

Hepatocellular carcinoma (HCC) is the sixth most common cancer and the third leading cause of cancer death worldwide (*1*). Despite the increasing prevalence of HCC and the fact that many patients present with advanced disease, there is a startling lack of treatments (*2*). Fortunately, recent studies suggested that successful targeted therapy could improve outcomes for HCC, even in the late stages of carcinogenesis, and may be the best choice for curative treatment. Sorafenib, a multi-kinase inhibitor, can effectively prolong the median overall survival of patients with advanced HCC from 8 to 11 months (*3*). However, Sorafenib was the sole targeted therapy approved for treating advanced HCC until 2016 (*4*). Many new targeted drugs, such as cabozantinib, regorafenib, ramucirumab, and lenvatinib that can inhibit multi-kinase or angiogenic factors have improved clinical outcomes for patients, but improvements in survival are still modest. Moreover, some of these drugs, like ramucirumab, might fail in subsequent clinical trials when the compound fails to result in effective improvements in overall survival for patients. Hence, identifying more underlying gene targets for initiation and progression of liver cancer is still urgently needed.

[§]These authors contributed equally to this work.
**Address correspondence to:*
Dr. Xiangwei Meng, Department of Gastroenterology, First Hospital of Jilin University, Changchun 130021, China.
E-mail: xiangweimeng2003@163.com

Dr. Lijing Zhao, Department of Recovery, Nursing School of Jilin University, Changchun 130021, China.
E-mail: Zhao_lj@jlu.edu.cn

Retinoid-interferon-induced mortality-19 (GRIM-19), an encoded protein localized in the nucleus, mitochondria, and cytoplasm, has been identified as a suppressor in various types of malignancies (*5*). GRIM-19 expression is also reported to be down-regulated in many carcinomas, such as colon cancer, breast cancer, ovarian cancer, and HCC (*6-9*). Over the past 2 decades, an increasing number of studies have indicated that GRIM-19 repressed tumors by inducing apoptosis, arresting the cell cycle, and inhibiting metastasis (*10-12*). In a previous study by the current authors, GRIM-19 was expressed at low levels in 54 HCC samples, and it suppresses liver cancer cell growth by inducing cell cycle arrest and promoting apoptosis in *in vitro* (*13*). Interestingly, the inhibitory effect of GRIM-19 on the signal transducer and activator of transcription 3 (Stat3) has been considered to be the potent mechanism by which GRIM-19 induces antitumor action (*14*).

Stat3, a multifaceted growth mediator in cells, has been recognized as a promoter in many malignancies, including HCC (*15*). In contrast, GRIM-19 was suggested to be a stronger inhibitor of Stat3 activation. Several studies indicated that GRIM-19 could repress the invasion and epithelial mesenchymal transition (EMT) of colorectal cancer *via* inactivation of Stat3 (*8,16*). Other studies reported that a low level of GRIM-19 expression directly induced Stat3 activation in many carcinomas (*6,7,9*). However, the mechanisms of low levels of GRIM-19 expression in carcinomas and the underlying the effects of GRIM-19 on tumorigenesis are still poorly understood. Nowadays, most studies are focusing on targeting carcinogenic molecules that may also be the essential for cell survival in normal organs, and this may cause adverse reactions. The aim here is to develop a strategy that up-regulates GRIM-19 expression using *Salmonella typhimurium* in HCC, a approach that has yet to be tested, as a potential therapy for HCC that causes fewer adverse reactions.

The current study created a mouse model of an orthotopically implanted hepatocarcinoma tumor to observe the effect of GRIM-19 on the growth of the xenografts, and it used an attenuated S. Typhimurium strain to deliver a GRIM-19 expression plasmid to the implanted HCC. In addition, this study also analyzed the expression of Stat3 and its downstream target genes in the xenograft to explore potential mechanisms of GRIM-19 action in tumorigenesis.

2. Materials and Methods

2.1. *Cells and animals*

A murine H22 ascites-derived, hepatocellular carcinoma cell line was donated by the Prostate Disease Research Center, Jilin University (China). Cells were routinely grown in the intraperitoneal space of C57BL/6 mice and then cryopreserved in liquid nitrogen. Inbred male C57BL/6 mice, weighing 18-22 g and ranging from 5-6 weeks of age, were purchased from the animal center of the School of Basic Medicine, Jilin University (China). All mice were housed at a constant temperature and constant humidity in a specific pathogen-free environment with free access to food and water. The study protocol was approved by the local ethics committee.

2.2. *Strains and plasmid*

The eukaryotic expression plasmid pcDNA3.1-GRIM-19 and empty vector pcDNA3.1 were donated by Dr. Hu JD of the University of Maryland (Baltimore, USA). The attenuated *S. Typhimurium* phoP/phoQ mutant strain PQ was stored by the Prostate Disease Research Center, Jilin University (China). Plasmids were electroporated into *Salmonella* to form the recombinant *Salmonella*e, which was then maintained at -80℃ in glycerol.

2.3. *Creation of an orthotopically implanted hepatocarcinoma tumor model*

C57BL/6 mice were subcutaneously inoculated with 0.1 mL (2×10^8 cells per mL) of suspended H22 cells to form a xenograft. When tumors reached 5 mm in diameter under the right axilla of the mice, they were removed and sliced into small pieces of 1 mm3 under sterile conditions. While mice were under anesthesia, the right lobe of the liver was punctured to form a 2-mm-long sinus tract, and a small piece of tumor tissue was inserted into each sinus tract, thus creating a model of orthotopically transplanted HCC tumors.

2.4. *Antitumor activity of GRIM-19 on xenografts*

When the xenografts reached 500 mm^3 in volume in the left lobe of the liver, they were deemed to be the standard model. Standardized mice with HCC xenograph implants were then randomly divided into three groups (n = 20 per group). Before each treatment, all mice were fasted overnight and orally pre-administered 100 μL of 10 g/L $NaHCO_3$ solution. Half an hour later, the Mock group was orogastrically inoculated with 100 μL of PBS, the PQ-Scramble group was similarly inoculated with 1×10^8 cfu of PQ-Scramble, and the PQ-GRIM-19 group was similarly inoculated with 1×10^8 cfu of PQ-GRIM-19. Treatments were administered once every 10 days for a total of two doses. The volume of orthotopic transplantation tumors was monitored using the Vevo770 High-Resolution Imaging System. The mice were sacrificed 21 days after the first treatment, and the tumors were excised, weighed, and photographed. Two hundred mg of fresh tumor tissue was collected to extract total protein and analyze the cell cycle and apoptosis; the remaining tissues were fixed in 4% paraformaldehyde for

morphological assays, immunohistochemical staining, and TUNEL staining.

2.5. *Western blot analysis*

Soluble proteins were extracted from 100 mg of tumor tissues and subjected to SDS-polyacrylamide gel electrophoresis. Separated proteins were electrophoretically transferred onto polyvinylidene difluoride (PVDF) membranes (Thermo Fisher Inc., Rockford, IL, USA) and immunoblotted with anti-GRIM-19, anti-CyclinD1, anti-β-actin, anti-PCNA, anti-Stat3, anti-p-Stat3(Tyr705), anti-Bax, anti-Bcl-2 or anti-cleaved caspase-9, anti-MMP-2, anti-MMP-9, anti-VEGF, anti-cleaved caspase-3 (C-Caspase-3), anti-CDK4, or anti-β-actin (Cell Signaling Technology, USA) overnight at 4℃ and then incubated with horseradish peroxidase (HRP)-tagged second antibody at room temperature for 1 hour. Finally, the protein level was detected with an ECL plus kit (Millipore, USA) and developed *via* the Odyssey Infrared Imaging System (Li-Cor, Lincoln, NE, USA) in accordance with the manufacturer's instructions.

2.6. *Analysis of the cell cycle*

Fifty mg of fresh tumor tissue was homogenized and suspended in RPMI-1640 with 10% FBS (Hyclone, USA). After centrifugation, cells were resuspended in RPMI-1640 with 10% FBS. Cells were collected at a density of 10^6 cells/mL in the presence of propidium iodide (PI) and RNase, both at a final concentration of 50 μg/mL. After storage in the dark at 4℃ for 1 h, DNA content was determined using a flow cytometric analysis with a FACS can flow cytometer (Becton Dickinson, San Jose, CA, USA) as previously described (*9*). Cell cycle analysis was performed using the software Multicycle (Phoenix Flow Systems, Inc., San Diego, CA, USA).

2.7. *Immunohistochemistry assays*

Tumor specimens fixed in 10% formalin were embedded in paraffin and cut into 3mm-thick slides. The slides were soaked in sodium citrate buffer and heated in a microwave oven at 98℃ for 15 min for epitope retrieval. Endogenous peroxidase activity was blocked with a 3% hydrogen peroxide solution at 37℃ for 25 min. Non-specific binding was prevented by normal goat serum at room temperature for 20 min. Immunostaining of target proteins was performed using specific mouse monoclonal antibodies. Goat anti-mouse IgG conjugated with horseradish peroxidase was used as the secondary antibody. The staining procedure was carried out manually at 37℃ for 30 min, using the HRP-avidin complexing method. Reactive products were visualized with 3,3'- diaminobenzidene (DAB) as the chromogen, and the slides were counterstained with hematoxylin. The stained slides were analyzed and photographed with a microscope, and cellular brownish staining was scored as positive.

2.8. *Annexin V/PI apoptosis assay*

Fifty mg of sample was homogenized to detect apoptosis with annexin V/PI. Cells were scraped from the container and stained with annexin V-FITC and PI according to the manufacturer's instructions (Annexin V- FITC Apoptosis Detection Kit, Beyotime Institute of Biotechnology, China). In brief, cells were washed with PBS twice, suspended in 400 μL of binding buffer, and incubated with 5 μL FITC-labeled annexin V for 15 min and 15 μL PI for 5 min, successively, at 4℃ in the dark. Apoptotic cells were measured in the FACScan flow cytometer.

2.9. *TUNEL assay*

The TUNEL assay was performed using the TUNEL System kit (Promega, Madison, WI, USA) according to the manufacturer's protocol. Briefly, the cells were permeabilized with Proteinase K (20 μg/mL) at 37℃ for 2 min followed by addition of TUNEL in the dark at 37℃ for 1 h. The localized green fluorescence of apoptotic cells was visualized using fluorescence microscopy.

2.10. *Statistical analysis*

Data are expressed as the mean ± standard error. Statistical analyses were performed with SPSS17.0 using an analysis of variance (ANOVA) test. $p < 0.05$ was deemed to be statistically significant.

3. Results

3.1. *GRIM-19 overexpression inhibits the growth of xenografts*

To evaluate the effects of GRIM-19 on tumor growth *in vivo*, an orthotopically implanted xenograft model was created, and xenograft volume and tumor weight were monitored. As shown in Figure 1A, 6 mice survived 21 days after orally receiving PBS and 10 survived after similarly receiving after receiving PQ-Scramble. However, 16 mice in the group treated with PQ-GRIM-19 survived. The xenograft volume was measured with a Vevo770 High-Resolution Imaging System in live mice, and the weight of excised tumors in the PQ-GRIM-19 group decreased significantly ($p < 0.05$) compared to that in the Mock and PQ-Scramble groups (Figure 1B, C and D).

To indicate that GRIM-19 had been transferred into the tumor tissues by the recombinant *S. Typhimurium*, a Western blot assay was used to detect protein expression in xenograft tissues. Importantly, the expression of

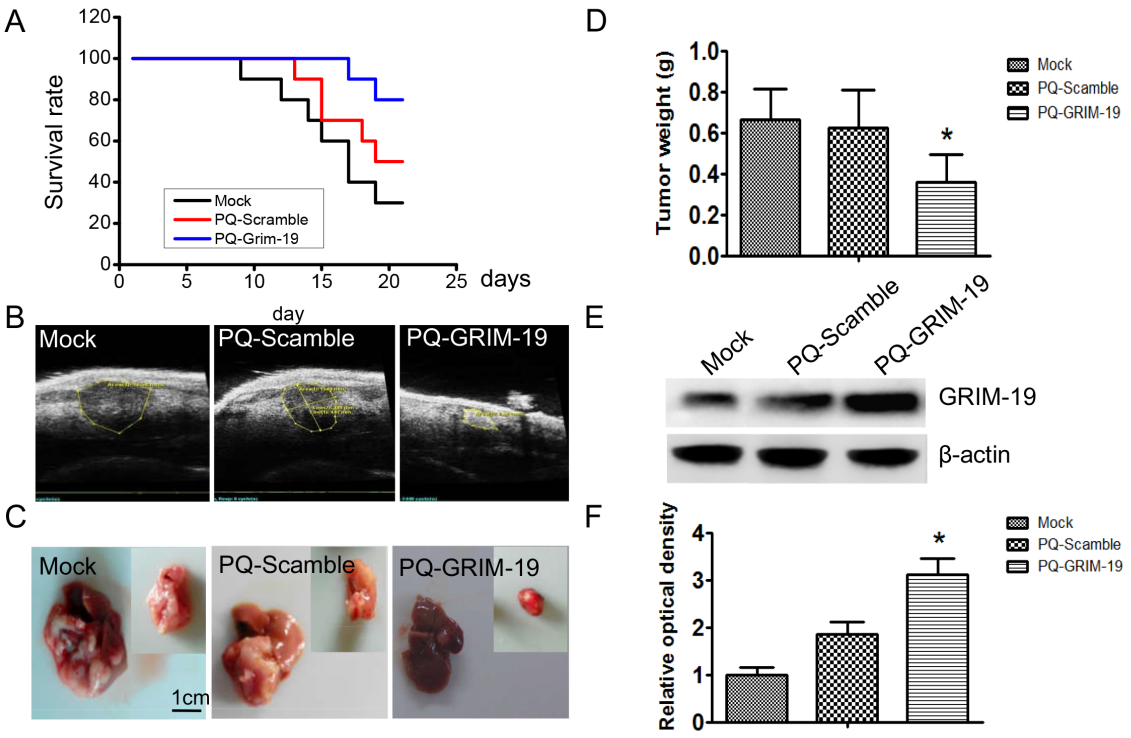

Figure 1. GRIM-19 overexpression inhibited H22 xenograft growth and increased the survival rate of mice with HCC. **(A)** Survival curves of mice bearing an orthotopically implanted hepatocarcinoma tumor following treatment with PQ-GRIM-19. **(B)** Tumor diameters measured with the Vevo770 High-Resolution Imaging System. **(C)** Representative livers and tumors were removed from mice. **(D)** Tumor weight. **(E)** GRIM-19 expression analyzed using Western blot analysis. **(F)** The relative optical density (OD) value for GRIM-19 according to Western blot analysis is shown in part E above.

GRIM-19 in the PQ-GRIM-19 group was significantly higher ($p < 0.05$) than that in the Mock and PQ-Scramble groups (Figure 1E and F). These results indicate that the overexpression of GRIM-19 can inhibit xenograft growth and enhance survival rates of tumor-bearing mice.

3.2. *GRIM-19 inhibits cell cycling, induces apoptosis, and inhibits metastasis of xenografts*

To study the mechanism by which GRIM-19 inhibits HCC growth, cell cycle, apoptosis, and metastasis were examined. Flow cytometric analysis indicated that the cells in PQ-the GRIM-19 group were mostly in the G0-G1 phase, whereas the proportion of cells in S the phase decreased significantly ($p < 0.05$) compared to that in the two control groups. These results suggest that GRIM-19 overexpression may suppress xenograft cell growth by arresting tumor cells in the G0-G1 phase (Figure 2A and B).

The cells were subjected to Annexin V-FITC/PI double staining and TUNEL staining to detect apoptosis. Results revealed that the rate of apoptosis in the PQ-GRIM-19 group was significantly higher ($p < 0.05$) than that in the control groups (Figure 2C, D and E).

Body weight was determined to evaluate ascites formation. There was no significant difference in weight in the Mock and PQ-Scramble groups, but weight was significantly lower in the PQ-GRIM-19 group ($p < 0.05$) compared to that in the two control groups (Figure 2F and G). Remarkably, abdominal tumor metastasis was observed in the Mock and PQ-Scramble groups (Figure 2H).

3.3. *GRIM-19 regulates expression of cell cycle-related proteins in xenografts*

To elucidate the mechanisms by which exogenous GRIM-19 mediated cell cycle arrest in transplantation tumor cells, Western blot analysis was used to examine the expression of cell cycle-related proteins (CDK4, PCNA and CyclinD1). Results indicated no significant difference in the expression of those proteins between the Mock and PQ-Scramble groups., CDK4, PCNA, and CyclinD1 expression were significantly down-regulated in the PQ-GRIM-19 group ($p < 0.05$) compared to levels in control cells (Figure 3A and B). These results were confirmed by immunohistochemical staining (Figure 3C), suggesting that the efficient induction of G0-G1 arrest by exogenous GRIM-19 over-expression was probably associated with the down-regulation of CDK4, PCNA, and CyclinD1 expression.

3.4. *GRIM-19 regulates apoptosis-related protein expression in xenografts*

To further explore the mechanism of cell apoptosis

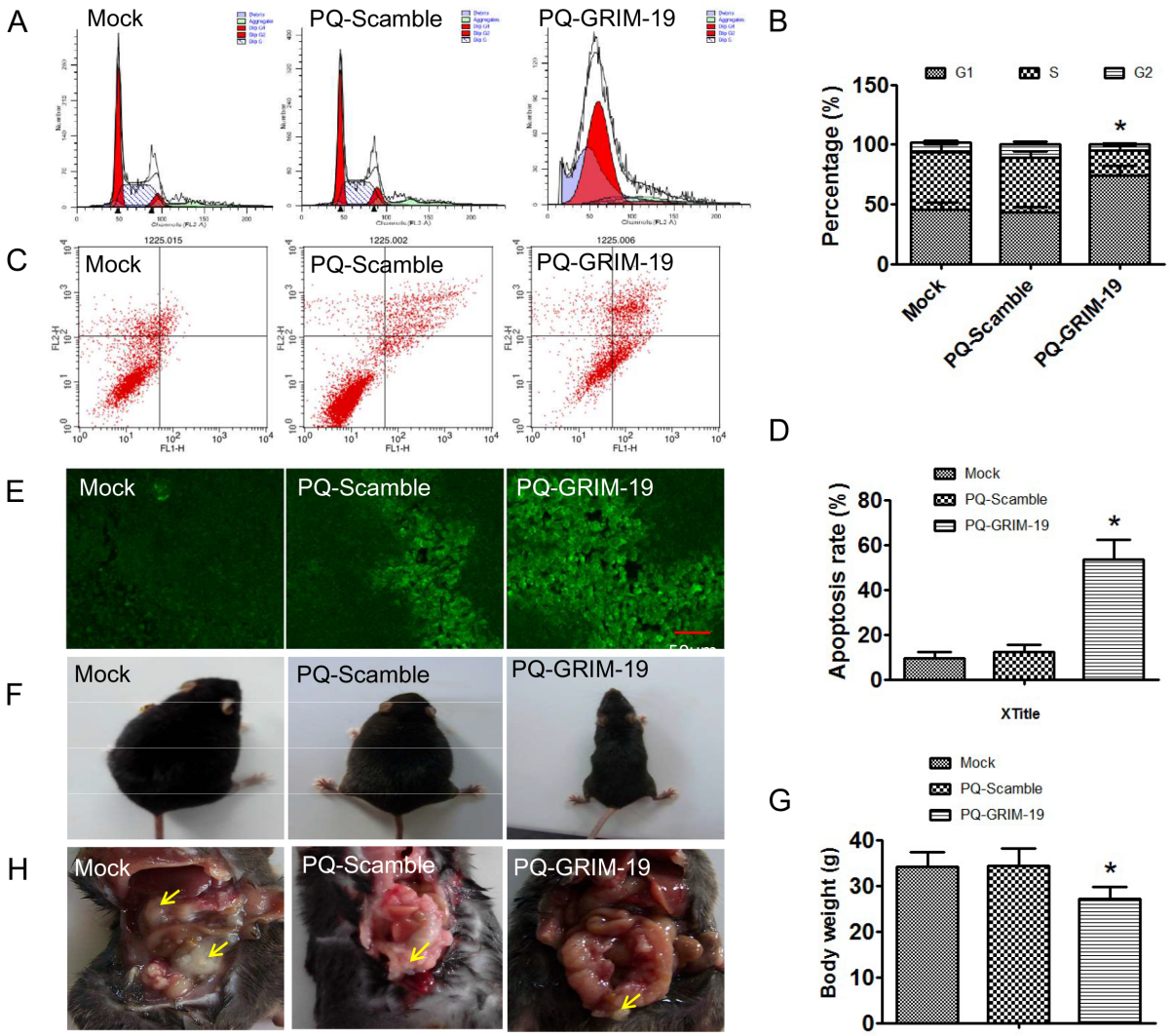

Figure 2. GRIM-19 overexpression induced G1/S arrest, enhanced apoptosis, and suppressed tumor metastasis. (A) FCM data with PI staining for cell cycle arrest. **(B)** Values represent the percentage of cells in each phase of the cell cycle. **(C)** Representative FCM data with Annexin-V-FITC and PI staining for cell apoptosis. **(D)** The average rate of cell apoptosis. **(E)** Analysis of late apoptosis in H22 xenografts with TUNEL fluorescent staining. **(F)** The appearance of mice, showing the extent of ascites formation. **(G)** Average body weight of mice. (H) The formation of abdominal metastases. Arrows indicate the location of tumors.

induced by exogenous GRIM-19, Bcl-2 family proteins Bax and Bcl-2 and caspase family proteins Caspase-3 and Caspase-9 were examined using Western blot analysis. Cells treated with PBS and the empty vector served as negative controls. As shown in Figure 4A and B, exogenous GRIM-19 significantly increased ($p < 0.05$) pro-apoptotic protein Bax expression and significantly down-regulated ($p < 0.05$) anti-apoptotic protein Bcl-2 expression in xenograft cells. Moreover, cleaved Caspase-3 and cleaved Caspase-9 were significantly were upregulated ($p < 0.05$) in the PQ-GRIM-19 group. In accordance with these results, the cells transfected with exogenous GRIM-19 tended to stain more positively for Bax, cleaved caspase-3, and cleaved caspase-9 and weaker for Bcl-2 compared to the negative controls (Figure 4C). These results indicate that tumor cell apoptosis induced by exogenous GRIM-19 was mediated by activation of the mitochondrial apoptosis pathway.

3.5. *GRIM-19 regulates metastasis-related protein expression in xenografts*

To study the molecular mechanisms for inhibition of tumor metastasis by GRIM-19 over-expression, VEGF, MMP9, and MMP2 proteins, which are involved in tumor metastasis, were monitored using Western blot analysis and immunohistochemical assays. As shown in Figure 5, these proteins were significantly down-regulated in the PQ-GRIM-19 group compared to levels in the control groups, revealing that GRIM-19 over-expression could inhibit tumor metastasis into the abdominal cavity by decreasing expression of VEGF, MMP9, and MMP2 proteins.

3.6. *GRIM-19 regulates the Stat3 signaling pathway*

To further elucidate the molecular mechanisms by

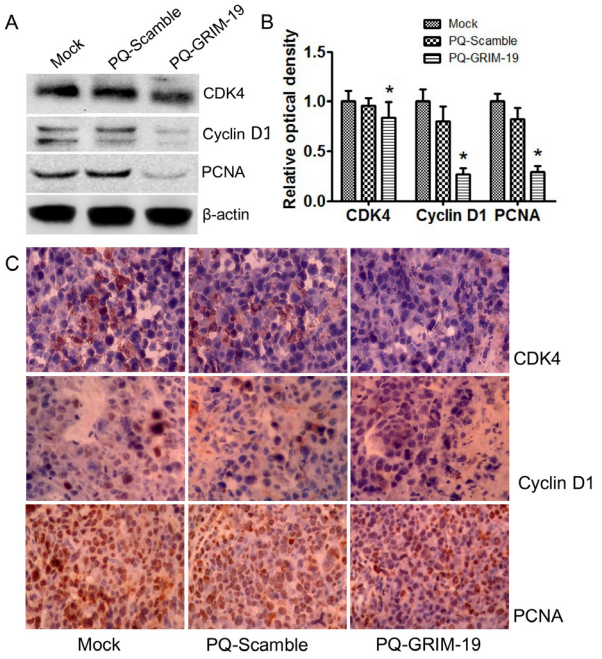

Figure 3. The effects of exogenous GRIM-19 on the expression of CyclinD1, CDK4, and PCNA. (A) Western blot assay for expression of CyclinD1, CDK4, and PCNA proteins. **(B)** Relative optical density (OD) value from Western blot analysis. **(C)** The xenograft tissues were immunostained for CyclinD1, CDK4, and PCNA with corresponding antibodies.

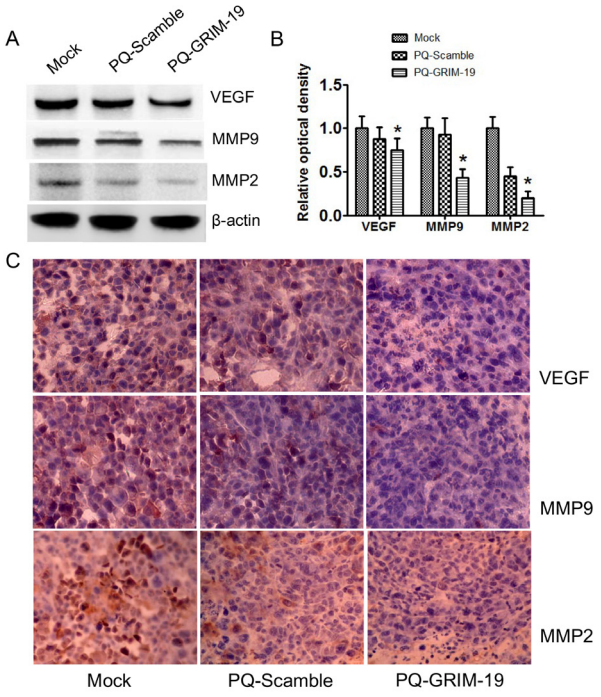

Figure 5. The expression of proteins associated with the inhibition of cell metastasis in xenografts. (A) Western blot assay for expression of VEGF, MMP-9, and MMP-2 proteins in xenografts. **(B)** Relative optical density (OD) value from each group according to Western blot analysis. **(C)** The same treated tumor xenograft tissues were immunostained for VEGF, MMP-9, and MMP-2 with corresponding antibodies.

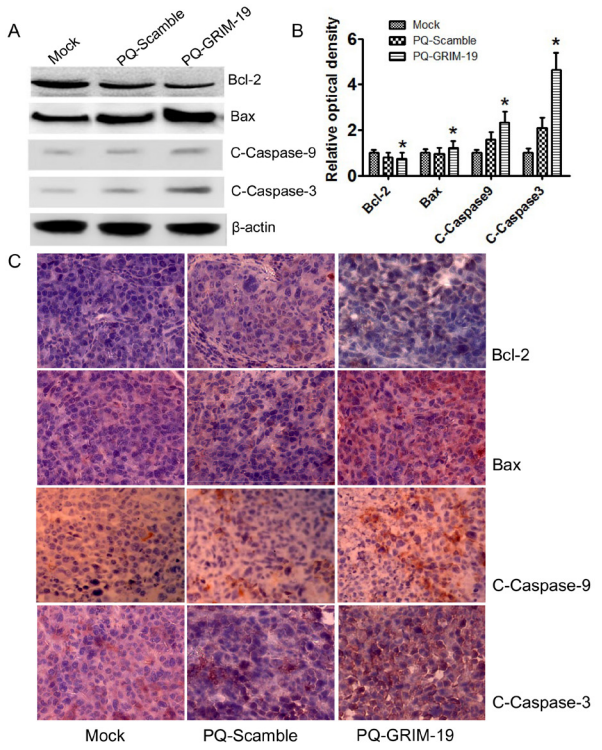

Figure 4. Exogenous GRIM-19 activates the mitochondrial apoptosis pathway. (A) Western blot assay for expression of Bax, Bcl-2, cleaved caspase-3 (C-Caspase-3), and cleaved caspase-9 (C-Caspase-9) proteins in xenografts. **(B)** Relative optical density (OD) values from Western blot analysis. **(C)** The xenograft tissues were immunostained for Bax, Bcl-2, C-Caspase-3, and C-Caspase-9 with corresponding antibodies.

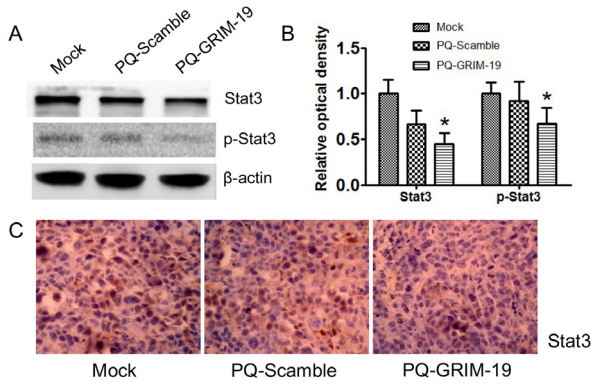

Figure 6. The expression of Stat3/ p-Stat3 proteins in xenografts. (A) Western blot analysis of Stat3/ p-Stat3. **(B)** Relative optical density (OD) value from Western blot analysis. **(C)** The xenograft tissues were immunostained for Stat3 with corresponding antibodies.

which GRIM-19 inhibits metastasis and induces apoptosis in HCC xenograft cells, this study investigated GRIM-19's effects on Stat3 protein expression and phosphorylation, which is a key process in this signaling pathway. As shown in Figure 6A and B, Western blot analyses indicated that exogenous GRIM-19 significantly decreased ($p < 0.05$) Stat3/p-Stat3 expression. Immunohistochemical assays revealed Stat3 down-regulation in cells treated with PQ-GRIM-19 compared to control cells (Figure 6C). These findings

suggest that GRIM-19 may restrict tumor cell growth and metastasis by negatively regulating the JAK/Stat signaling pathway.

4. Discussion

An increasing number of genes essential for normal tissue/organ growth and development have been identified as being involved in HCC (*17,18*). Studies have indicated that malignancies are closely related to genes that affect cellular differentiation, development, and senescence during normal growth. Tumorigenesis of various cancer types is reported to be closely associated with GRIM-19 gene mutation or dysfunction (*8,19,20*). A previous study by the current authors indicated that GRIM-19 expression was down-regulated in most HCC samples in contrast to adjacent non-tumor liver tissues and that over-expression of GRIM-19 suppressed tumor cell growth by inducing cell cycle arrest and promoting apoptosis *in vitro* (*13*). The current study created a mouse model of an orthotopically implanted hepatocarcinoma tumor to verify the effect on tumor suppression of GRIM-19 over-expression *in vivo* and to discuss its mechanism.

Unlike conventional chemotherapeutic drugs, gene-targeted therapies are theoretically more effective in tumor eradication, and less harmful to normal cells, because specific molecular mechanisms are involved (*21*). However, the "Achilles heel" of gene-targeted therapy is vector deficiency. *Salmonella typhimurium*, a type of facultative anaerobic Gram-negative bacteria, can selectively accumulate in solid tumors because of the existence of hypoxic areas within solid tumors (*22*). Attenuated Salmonella phoPphoQ was used in the current study as a GRIM-19-expressing plasmid carrier because of its potent tumor-targeting ability, low toxicity, and ability to efficiently express exogenous gene products (*23*). Several studies have indicated that GRIM-19 expressing plasmids in *phoPphoQ Salmonella* can target solid tumors and be released into implanted tumor cells to successfully over-express GRIM-19 protein.

This study used PQ-GRIM-19, and results indicated that over-expressed GRIM-19 resulted in an increase in the survival rate of mice with HCC and a decrease in tumor volume, ascites, and abdominal metastases, indicating that the growth of orthotopical xenografts was suppressed by over-expressed GRIM-19. These results mirrored those of a previous study by the current authors (*24*).

Although the mechanisms of the anti-tumor actions of GRIM-19 are not completely clear, researchers have often stressed that GRIM-19's function as a tumor inhibitor involves multiple factors. CDK4 and cyclin D1 are important factors during the cell cycle. GRIM-19 can induce G1/S arrest of cancer cells by down-regulating CDK4 and cyclinD1 (*5,10,25*). In the current study, the up-regulation of GRIM-19 causing the decrease in CDK4 and cyclinD1 might have led to a significant arrest of xenograft cells in G1/S, as previously described. PCNA, a nuclear protein localized at active replication sites, is reported to contribute to DNA replication and repair during the S phase (*26,27*). The current results implied that GRIM-19 overexpression efficiently prevents transition from the G1 to S phase by reducing CDK4 and CyclinD1 protein expression, ultimately leading to the decrease in PCNA *in vivo*. Those results were consistent with results when using SMMC-7721 cells *in vitro* (*13*). Accordingly, the hypothesis is that GRIM-19 can suppress the replication and repair of damaged DNA by inducing G1/S arrest, so GRIM-19 could help to limit uncontrolled cancer cell proliferation.

The mitochondria apoptosis pathway reportedly plays a key role in the process of apoptosis and served as a natural barrier to cancer development (*28*). Interestingly, GRIM-19 was originally identified as a nuclear protein affecting mitochondrial apoptosis in interferon/retinoic acid-induced tumor cell death (*11*). The participation of mitochondria in apoptosis was relevant to Bcl-2 family members that triggered apoptosis by regulating the permeability of mitochondrial membranes (*29*). The relative balance of various pro-apoptotic (Bax, Bad) and anti-apoptotic (Bcl-2, Bcl-xL, Bcl-w, and Mcl-1) Bcl-2 family members was a critical cellular homeostasis mechanism. Cleaved-caspase-9 and cleaved-caspase-3 can trigger the caspase cascade and process of apoptosis. The current study revealed that GRIM-19 overexpression promoted apoptosis by increasing the Bax/Bcl-2 ratio and cleaved caspase-3 and cleaved caspase-9. Analogous results have been observed in lung cancer and glioma (*12,30*), suggesting that GRIM-19 induces apoptosis *via* activation of the mitochondria apoptosis pathway.

In addition to suppressing growth, GRIM-19 inhibits the metastasis of hepatocarcinoma tumor cells. Several studies have claimed that down-regulation of GRIM-19 correlates with invasive features of breast cancer, glioma, and HCC (*7,12,31*). A study by the current authors indicated that treatment of tumor-bearing mice with PQ-GRIM-19 for 10 days led to an appreciable decrease in vascular endothelial growth factor (VEGF) and matrix-degrading enzyme metalloproteinase-2 (MMP-2) and MMP-9 activity, findings which were similar to those of a study of gastric cancer (*32*). MMP-9 and MMP-2 play crucial roles in regulating cancer cells invasion and metastasis (*33*). VEGF reportedly contributes to an increase in the invasive potential in colorectal cancer (34). A reduction in MMP-2 and VEGF could inhibit angiogenesis-mediated human hepatocellular metastasis (*35*). Thus, preventing upregulation of VEGF, MMP-2, and MMP-9 by PQ-GRIM-19 treatment might be a potential strategy to render HCC less invasive.

Several studies have indicated that signal transducers and activators of transcription 3 (Stat3), a key controller of the JAK/Stat signaling pathway, are involved in carcinogenesis by promoting cell proliferation, differentiation, and cell cycle progression, as well as by inhibiting apoptosis. Indeed, constitutive activation of Stat3 705 tyrosine phosphorylation and its up-regulation have been observed in diverse human tumors, including gliomas, as well as in prostate and thyroid cancers (*12,36*). Recent studies have indicated that Stat3 activation can accelerate tumor progression and metastasis, prolong cell survival, and inhibit cell apoptosis by incessantly regulating its downstream target genes, such as Bcl-2, Bax, Cyclin D1, MMP-2, and MMP-9 (*36*). Importantly, a previous study indicated that GRIM-19 was suppressed in HCC tissues, with a corresponding increase in p-Tyr(705)-Stat3 (p-Stat3) activity (*6*). These results might indicate a delicate relationship between GRIM-19 deactivation and Stat3 activation. GRIM-19 might regulate Stat3 and p-Stat3 expression and then mediate cell cycle progression, cell apoptosis, and cell migration. To verify this contention and to further investigate the possible mechanisms by which GRIM-19 inhibits growth, GRIM-19's effects on Stat3/p-Stat3 protein in xenograft tissues were examined. The data in this study suggest that exogenous GRIM-19 down-regulated Stat3 expression and phosphorylation, implying that GRIM-19 might inversely regulate Stat3 signaling in HCC.

In summary, a mouse model of orthotopically implanted HCC tumors has demonstrated that GRIM-19 acts as a regulator that induces G1/S arrest, suppresses tumor cell migration, and promotes tumor apoptosis *in vivo*. Furthermore, evidence indicates that GRIM-19 inhibits Stat3 expression and phosphorylation, which apparently deactivate the Stat3 signaling pathway and then inhibit tumor growth. The mechanism by which GRIM-19 affects Stat3 expression and phosphorylation remains undetermined. GRIM-19 apparently affects hepatocarcinogenesis at multiple levels and could be a potential therapy for HCC. Administration of GRIM-19 carried by attenuated *S. Typhimurium* could be a novel and targeted strategy with which to treat hepatocellular cancer.

Acknowledgements

This study was support by the Zhejiang Medical and Health Science and Technology Project (grant no. 2018254697).

References

1. Bray F, Ferlay J, Soerjomataram I, Siegel RL, Torre LA, Jemal A. Global cancer statistics 2018: GLOBOCAN estimates of incidence and mortality worldwide for 36 cancers in 185 countries. CA Cancer J Clin. 2018; 68:394-424.
2. Gravitz L. Liver cancer. Nature. 2014; 516:S1.
3. Tong Z, Zhou Y, Wang J. Identifying potential drug targets in hepatocellular carcinoma based on network analysis and one-class support vector machine. Sci Rep. 2019; 9:10442.
4. Llovet JM, Montal R, Sia D, Finn RS. Molecular therapies and precision medicine for hepatocellular carcinoma. Nat Rev Clin Oncol. 2018; 15:599-616.
5. Wu N, Hui H, Cui L, Yang F. GRIM-19 represses the proliferation and invasion of cutaneous squamous cell carcinoma cells associated with downregulation of STAT3 signaling. Biomed Pharmacother. 2017; 95:1169-1176.
6. Li F, Ren W, Zhao Y, Fu Z, Ji Y, Zhu Y, Qin C. Downregulation of GRIM-19 is associated with hyperactivation of p-STAT3 in hepatocellular carcinoma. Med Oncol. 2012; 29:3046-3054.
7. Zhou T, Chao L, Rong GH, Wang CG, Ma R, Wang X. Down-regulation of GRIM-19 is associated with STAT3 overexpression in breast carcinomas. Hum Pathol. 2013; 44:1773-1779.
8. Zhang J, Chu D. GRIM-19 repressed hypoxia-induced invasion and EMT of colorectal cancer by repressing autophagy through inactivation of STAT3/HIF-1alpha signaling axis. J Cell Physiol. 2019; 234:12800-12808.
9. Ilelis F, do Amaral NS, Alves MR, da Costa A, Calsavara VF, Lordello L, De Brot L, Soares FA, Rodrigues IS, Rocha RM. Prognostic value of GRIM-19, NF-kappaB and IKK2 in patients with high-grade serous ovarian cancer. Pathol Res Pract. 2018; 214:187-194.
10. Saeid S, Mahmoud A, Mahdi S, Mojtaba F, Majid S, Marzieh M. Adenosine induces cell cycle arrest and apoptosis *via* cyclinD1/Cdk4 and Bcl-2/Bax pathways in human ovarian cancer cell line OVCAR-3. Tumor Biol. 2013; 34:1085-1095.
11. Chomova M, Dobrota D, Racay P. Ischemia-induced inhibition of mitochondrial complex I in rat brain: Effect of permeabilization method and electron acceptor. Neurochem Res. 2012; 37:965-976.
12. Yanmin Z, Hongbo H, Shidou Z, Qian L, Qiuhuan Y, Shilei N, Fuwu W, Shangming L, Liyan W, Aijun H. Downregulation of GRIM-19 promotes growth and migration of human glioma cells. Cancer Sci. 2011; 102:1991-1999.
13. Dexia K, Lijing Z, Yanwei D, Ping H, Yabin Z, Luoluo Y, Liankun S, Hebin W, Deqi X, Xiangwei M. Overexpression of GRIM-19, a mitochondrial respiratory chain complex I protein, suppresses hepatocellular carcinoma growth. Int J Clin Exp Pathol. 2014; 7:7497-7507.
14. Chengchen L, Jing M, Guochang H, Tong Z, Veronica ND, Chin Thing O, Xinmin C. GRIM-19, a death-regulatory gene product, suppresses Stat3 activity *via* functional interaction. EMBO J. 2014; 22:1325-1335.
15. Wu WY, Li J, Wu ZS, Zhang CL, Meng XL. STAT3 activation in monocytes accelerates liver cancer progression. BMC Cancer. 2011; 11:506-506.
16. Yun H, Lin Z, Haiyang X, Weilin W, Shusen Z. Differences in antiproliferative effect of STAT3 inhibition in HCC cells with versus without HBV expression. Biochem Biophys Res Commun. 2015; 461:513-518.
17. Hu G, Yan Z, Zhang C, Cheng M, Yan Y, Wang Y, Deng L, Lu Q, Luo S. FOXM1 promotes hepatocellular carcinoma progression by regulating KIF4A expression. J Exp Clin Cancer Res. 2019; 38:188.

18. Lin J, Shi J, Guo H, *et al*. Alterations in DNA damage repair genes in primary liver cancer. Clin Cancer Res. 2019; 25:4701-4711.
19. Zender L, Villanueva A, Tovar V, Sia D, Chiang DY, Llovet JM. Cancer gene discovery in hepatocellular carcinoma. J Hepatol. 2010; 52:921-929.
20. Yue X, Zhao P, Wu K, Huang J, Zhang W, Wu Y, Liang X, He X. GRIM-19 inhibition induced autophagy through activation of ERK and HIF-1alpha not STAT3 in Hela cells. Tumour Biol. 2016; 37:9789-9796.
21. Reyes-Habito CM, Roh EK. Cutaneous reactions to chemotherapeutic drugs and targeted therapy for cancer: Part II. Targeted therapy. J Am Acad Dermatol. 2014; 71:217.e211-217.e211; quiz 227-218.
22. Liu Z, Liu X, Cao W, Hua ZC. Tumor-specifically hypoxia-induced therapy of SPRY1/2 displayed differential therapeutic efficacy for melanoma. Am J Cancer Res. 2015; 5:792-801.
23. Liu YB, Zhang L, Guo YX, Gao LF, Liu XC, Zhao LJ, Guo BF, Zhao LJ, Zhao XJ, Xu DQ. Plasmid-based Survivin shRNA and GRIM-19 carried by attenuated Salmonella suppresses tumor cell growth. Asian J Androl. 2012; 14:536-545.
24. Liu S, Zhang W, Liu K, Wang Y, Ji B, Liu Y. Synergistic effects of co-expression plasmid-based ADAM10-specific siRNA and GRIM-19 on hepatocellular carcinoma *in vitro* and *in vivo*. Oncol Rep. 2014; 32:2501-2510.
25. Sun P, Nallar SC, Raha A, Kalakonda S, Velalar CN, Reddy SP, Kalvakolanu DV. GRIM-19 and p16(INK4a) synergistically regulate cell cycle progression and E2F1-responsive gene expression. J Biol Chem. 2010; 285:27545-27552.
26. Celis JE, Celis A. Cell cycle-dependent variations in the distribution of the nuclear protein cyclin proliferating cell nuclear antigen in cultured cells: Subdivision of S phase. Proc Natl Acad Sci U S A. 1985; 82:3262-3266.
27. Bartova E, Suchankova J, Legartova S, Malyskova B, Hornacek M, Skalnikova M, Masata M, Raska I, Kozubek S. PCNA is recruited to irradiated chromatin in late S-phase and is most pronounced in G2 phase of the cell cycle. Protoplasma. 2017; 254:2035-2043.
28. Miyabayashi T, Teo JL, Yamamoto M, McMillan M, Nguyen C, Kahn M. Wnt/beta-catenin/CBP signaling maintains long-term murine embryonic stem cell pluripotency. Proc Natl Acad Sci U S A. 2007; 104:5668-5673.
29. Birkinshaw RW, Czabotar PE. The BCL-2 family of proteins and mitochondrial outer membrane permeabilisation. Semin Cell Dev Biol. 2017; 72:152-162.
30. Wang T, Yan XB, Zhao JJ, Ye J, Jiang ZF, Wu DR, Xiao WH, Liu RY. Gene associated with retinoid-interferon-induced mortality-19 suppresses growth of lung adenocarcinoma tumor *in vitro* and *in vivo*. Lung Cancer. 2011; 72:287-293.
31. Hao H, Liu J, Liu G, Guan D, Yang Y, Zhang X, Cao X, Liu Q. Depletion of GRIM-19 accelerates hepatocellular carcinoma invasion *via* inducing EMT and loss of contact inhibition. J Cell Physiol. 2012; 227:1212-1219.
32. Huang Y, Yang M, Yang H, Zeng Z. Upregulation of the GRIM-19 gene suppresses invasion and metastasis of human gastric cancer SGC-7901 cell line. Exp Cell Res. 2010; 316:2061-2070.
33. Tauro M, Shay G, Sansil SS, Laghezza A, Tortorella P, Neuger AM, Soliman H, Lynch CC. Bone-seeking matrix metalloproteinase-2 inhibitors prevent bone metastatic breast cancer growth. Mol Cancer Ther. 2017; 16:494-505.
34. Araujo RF, Jr., Lira GA, Vilaca JA, Guedes HG, Leitao MC, Lucena HF, Ramos CC. Prognostic and diagnostic implications of MMP-2, MMP-9, and VEGF-alpha expressions in colorectal cancer. Pathol Res Pract. 2015; 211:71-77.
35. Park JY, Park DH, Jeon Y, Kim YJ, Lee J, Shin MS, Kang KS, Hwang GS, Kim HY, Yamabe N. Eupatilin inhibits angiogenesis-mediated human hepatocellular metastasis by reducing MMP-2 and VEGF signaling. Bioorg Med Chem Lett. 2018; 28:3150-3154.
36. Wang GM, Ren ZX, Wang PS, Su C, Zhang WX, Liu ZG, Zhang L, Zhao XJ, Chen G. Plasmid-based Stat3-specific siRNA and GRIM-19 inhibit the growth of thyroid cancer cells *in vitro* and *in vivo*. Oncol Rep. 2014; 32:573-580.

(Received July 21, 2019; Revised August 30, 2019; Accepted August 31, 2019)